

# Use of measuring gauges for *in vivo* accuracy analysis of intraoral scanners: a pilot study

Mikel Iturrate<sup>1\*</sup>, Xabier Amezua<sup>2</sup>, Xabier Garikano<sup>2</sup>, Eneko Solaberrieta<sup>2</sup>

<sup>1</sup>Department of Business Management, Faculty of Engineering Gipuzkoa, University of the Basque Country UPV/EHU, San Sebastian, Spain

<sup>2</sup>Department of Graphic Design and Engineering Projects, Faculty of Engineering Gipuzkoa, University of the Basque Country UPV/EHU, San Sebastian, Spain

## ORCID

Mikel Iturrate

<https://orcid.org/0000-0001-7113-7408>

Xabier Amezua

<https://orcid.org/0000-0003-2163-9957>

Xabier Garikano

<https://orcid.org/0000-0002-2228-7298>

Eneko Solaberrieta

<https://orcid.org/0000-0003-1734-2173>

**PURPOSE.** The purpose of this study is to present a methodology to evaluate the accuracy of intraoral scanners (IOS) used *in vivo*. **MATERIALS AND METHODS.** A specific feature-based gauge was designed, manufactured, and measured in a coordinate measuring machine (CMM), obtaining reference distances and angles. Then, 10 scans were taken by an IOS with the gauge in the patient's mouth and from the obtained stereolithography (STL) files, a total of 40 distances and 150 angles were measured and compared with the gauge's reference values. In order to provide a comparison, there were defined distance and angle groups in accordance with the increasing scanning area: from a short span area to a complete-arch scanning extension. Data was analyzed using software for statistical analysis. **RESULTS.** Deviations in measured distances showed that accuracy worsened as the scanning area increased: trueness varied from  $0.018 \pm 0.021$  mm in a distance equivalent to the space spanning a four-unit bridge to  $0.106 \pm 0.08$  mm in a space equivalent to a complete arch. Precision ranged from  $0.015 \pm 0.03$  mm to  $0.077 \pm 0.073$  mm in the same two areas. When analyzing angles, deviations did not show such a worsening pattern. In addition, deviations in angle measurement values were low and there were no calculated significant differences among angle groups. **CONCLUSION.** Currently, there is no standardized procedure to assess the accuracy of IOS *in vivo*, and the results show that the proposed methodology can contribute to this purpose. The deviations measured in the study show a worsening accuracy when increasing the length of the scanning area. [J Adv Prosthodont 2021;13:191-204]

## Corresponding author

Mikel Iturrate

UPV/EHU University of the Basque Country, Gipuzkoa Faculty of Engineering, Europa Plaza 1, 20.018 Donostia-San Sebastián, Spain

Tel +34 943 01 8661

E-mail [mikel.iturrate@ehu.eus](mailto:mikel.iturrate@ehu.eus)

Received April 5, 2021 /

Last Revision August 5, 2021 /

Accepted August 9, 2021

This study was supported by the MINECO Ministry of Economy and Competitiveness (grant number PID2019-108975RA-I00).

## KEYWORDS

Intraoral scanner; 3D optical scanner; Measuring gauge; *In vivo* accuracy evaluation; Digital impression

© 2021 The Korean Academy of Prosthodontics

© This is an Open Access article distributed under the terms of the Creative Commons Attribution Non-Commercial License (<http://creativecommons.org/licenses/by-nc/4.0>) which permits unrestricted non-commercial use, distribution, and reproduction in any medium, provided the original work is properly cited.

## INTRODUCTION

The development of a wide variety of optical scanners has enabled the capture of 3D images of the dental arches. These digital impressions are acquired by digitizing plaster models with laboratory scanners or by digitizing directly in the oral cavity, using intraoral scanners (IOS). The use of IOS is becoming increasingly common, and the manufacturers have developed more accurate devices; it is more comfortable for patients; digital workflows are more cost- and time-effective.<sup>1-4</sup> Nonetheless, conventional impression methods, where a dental arch replica in stone or plaster is manufactured, are still in wide use. One reason is because there is still doubt regarding the accuracy of 3D digital replicas obtained with these scanners, especially when digitizing long span areas such as the complete arch. In contrast, IOS show high accuracy when scanning short span areas such as a tooth or a bridge up to half an arch.<sup>5-8</sup>

When discussing non-contact scanners, whether for medical or industrial application, several sources of error have been reported. Some are specific to the equipment itself, such as the calibration procedure, the mathematical algorithms or the camera resolution.<sup>9,10</sup> External errors have also been reported: light conditions, surface roughness, the existence of liquid on the scanning surface, and scanning element colors influencing the scanning result.<sup>11-13</sup> These errors can also be attributable to IOS, as they are a type of non contact scanner.

In addition to the aforementioned errors inherent to the technology, the scanning of static elements under well controlled conditions is more favorable than scanning in a patient's mouth. During the patient-scanning procedure there are uncontrollable elements, such as the patient's movements, saliva, blood, interfering soft tissues, etc., that can adversely affect scan results.<sup>14-18</sup> Consequently, it is difficult for this technology to completely replace conventional methods in dentistry. Assuming all these difficulties, however, the eventual adoption of the IOS in clinics is inevitable.

The expectations created around this technology have led researchers worldwide to conduct studies in order to define the accuracy of IOS and to com-

pare their advantages or disadvantages with respect to conventional methods of obtaining dental impressions. Most research studies have been performed *in vitro* (with replicas of a patient's mouth or denture) and have analyzed different characteristics: the accuracy, the trueness or the precision of IOS on a single tooth, a bridge or in complete arch dental impressions.<sup>1,19-25</sup> Some studies, instead of measuring parameters related to the scanning device, such as accuracy, have evaluated the distance and angulation errors in specific clinical cases based on the use of external geometries such as screwed abutments or gauges.<sup>26,27</sup> In addition to *in vitro* studies, *in vivo* studies have also been conducted. These studies better represent the reality for which IOS have been designed and they have been performed on one tooth, dental arch quadrant or full arch following different methodologies. As in the studies performed *in vitro*, the published numerical values vary depending on the measured parameter or the methodology used.<sup>28-35</sup>

However, there is not yet an established protocol for assessing the accuracy of 3D optical scanners in general, nor one specific to IOS.<sup>10,36</sup> Being aware of the need for this, in 2015, the International Standardization Organization (ISO) recommended a protocol to standardize the accuracy of laboratory dental optical scanners using calibrated elements (ISO 12836: 2015 - Dentistry - Digitizing devices for CAD-CAM systems for indirect dental restorations - Test methods for assessing accuracy).<sup>37</sup> However, this standard establishes criteria for calculating the accuracy of scans in cases spanning distances ranging from a single tooth to the equivalent of a 4-unit bridge, but not for the complete arch and not for IOS.

IOS also require a standardized accuracy analysis protocol, and to this end, studies should be performed using feature-based gauges as suggested by ISO for laboratory scanners. Studies based on gauges to analyze both intraoral and laboratory scanners already exist<sup>27,35,36</sup> and this work presents an alternative in this area. The aim of the presented study is to prove the validity of a methodology to assess the accuracy of an IOS *in vivo*, by testing it in a real patient. This methodology and similar have already been tested *in vitro* and have provided trueness and precision values for different IOS.<sup>27,35,38</sup> In order to test the fea-

sibility of the proposed method, the validity of digital impressions ranging from small scan areas up to the complete dental arch were studied. From this, the proposed null hypothesis establishes that there are no significant differences between the accuracy of intraoral digital impressions of a short span area and in those of a complete arch.

## MATERIALS AND METHODS

The process was structured in three distinct phases. Phase one consisted of designing and manufacturing a gauge, to later be measured it in a coordinate measuring machine (CMM) to obtain the reference values. In the second phase, a patient's upper dental arch was scanned using an IOS, with the gauge placed in the patient's mouth. Finally, the digital replicas were measured using software for analyzing 3D measuring data to compare them with the reference values.

Three variables were taken into consideration for the design of the measuring gauge as a calibration element: 1) the size, so that it could be used in different individuals; 2) its validity to measure errors in distances and angles; and 3) the material, opting for one that was biocompatible. To meet the first condition, digital impressions of the maxilla of five individuals were obtained and aligned using Geomagic Control (3D Systems - 2018.1.1 software version, Rock Hill, SC, USA). Then, using Design X software (3D Systems - 2016.2.2 software version), the gauge was created to fit the space of the five aligned impressions. The design included the cylinders and the reference plane

needed to measure distances and angles. These cylinders were strategically positioned in regard to the oral cavity: they were positioned as close as possible to the dentition so that they could be scanned during the acquisition of the digital impressions; and they had to be located where hypothetical deformations may occur (in the incisor region, the curvature of the arch increases and simultaneously decreases the occlusal surface) and where the scanning procedure should begin and end, following the manufacturer's scanning protocols (Fig. 1). Finally, the gauge was fabricated using biocompatible stainless steel (316/316L) in a computer numerical control milling machine (CNC) and shot-blasted to avoid shiny surfaces that could impair the scanning process.

Then, the gauge was measured with a touch-trigger probe in a reference CMM (Crysta Apex S 9106, Mitutoyo, Kawasaki, Japan - Maximum permissible error  $E_{0, MPE} = (1.7 + 3L / 1000)\mu\text{m}$ ) obtaining four distances (D1, D2, D3, D4) and five angles (A1, A2, A3, A4, A5). The reference plane was initially defined by contact of the reference plane of the gauge. The process was followed by defining the cylinders and their axes. Each geometric feature was defined with 30 probe hits (Fig. 2). These axes were used to measure the angles with respect to the XY plane, and as intersection lines to define the points that were used to measure reference distances. The intersection plane was a virtual plane parallel to the reference plane and spaced 3 mm in height. Intersection points were created by intersecting cylinder axes and the virtual parallel plane. For further information on deviations in angle mea-

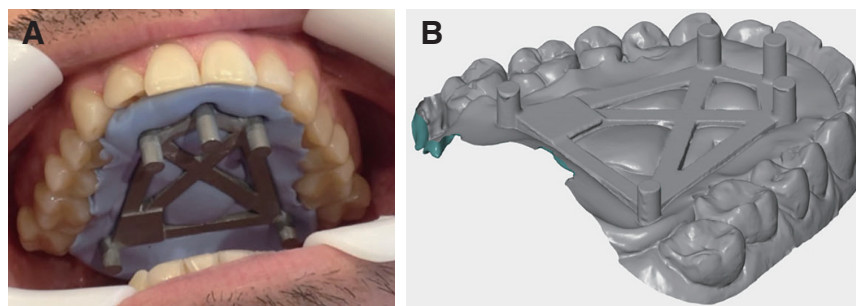


**Fig. 1.** (A) Gauge placed and fixed in the mouth, (B) digital impression acquired with the IOS.

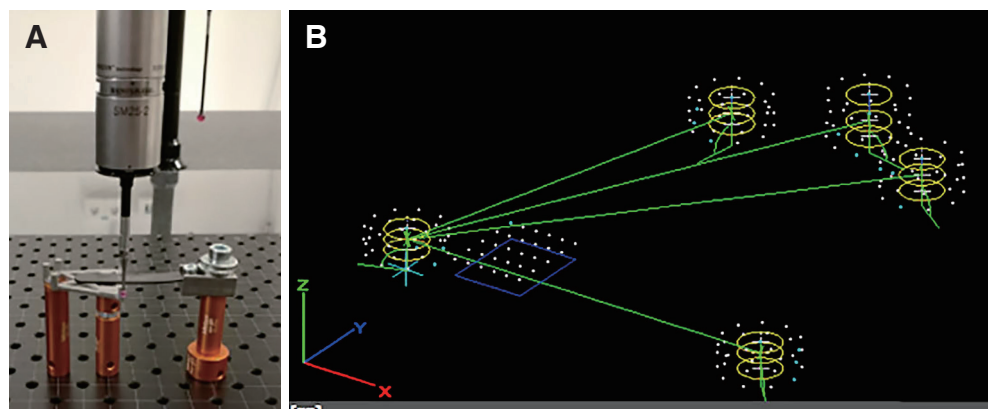


**Fig. 2.** (A) Gauge measurement in CMM, (B) geometric features definition with 30 probe hits in each.

surements, their projections in YZ and ZX planes were also calculated. All these measurements were used as reference.

In the second phase, 10 complete-arch scans were taken of a patient with the gauge in the mouth. The scanning began in the maxillary third molar region, digitizing the first cylinder, and continued along the arch, following the cylinders in numerical order until reaching the fifth cylinder and achieving digitization of the complete arch. This patient had a natural complete dentition and no pathologic diagnosis. He was recruited following the protocol approved by the institutional ethics committee (CEISH M10/2019/254, UPV-EHU) and in compliance with the requirements contained in the corresponding report. The gauge was fixed in the maxillary using light-polymerizing resin (CONLIGHT, Kuss Dental, Madrid, Spain). The resin was directly adhered to the patient's palate and the gauge was partially immersed in it before polymerization. Digital full-arch replicas were achieved with the IOS Cerec Omnicam (SW version 4.6, Dentsply Sirona, Charlotte, NC, USA) (STL1-STL10) (Fig. 1). The same dentist took all 10 digital impressions following the manufacturer's proposed scanning protocol.

The 10 digital impressions were exported as stereolithography (STL) files into GOM Inspect (GOM-2019 software version, Zeiss, Oberkochen, Germany), 3D inspection and mesh processing software. The same four distances, five angles and their projections in YZ and ZX as those assessed in the gauge as references were measured in each STL file.

After testing different measuring tools and procedures of GOM Inspect, a specific protocol was designed to perform the measurements. This protocol was followed for the measurement of all 3D meshes acquired with the IOS. Five digital cylinders and a plane (Plane 1, Fig. 3) were created in each STL file using a "Geometry-based" selection. For that purpose, it used the part of the mesh generated as the replica of the reference cylinders and reference plane of the gauge. The software (GOM Inspect) squares the deviations of the selected polygons with a possible fitting element using best-fit algorithms based on Gaussian approximation. Then, following the same procedure used to measure the gauge in the CMM, control distances were measured in the digital 3D replicas: an intersection plane (Plane 2) was built parallel to the reference plane (Plane 1) at 3 mm. Then, by intersecting Plane 2 and the axis of each digitally built cylinder, five intersection points were created (IP1-IP5). Reference distances were measured as distances between these intersection points (D1, D2, D3, D4) (Fig. 3). At all distances, the origin point was the first cylinder. This is the cylinder located where the arch scanning process began. The rest of the distances were equivalent to increasing lengths of scans reaching the full arch, represented by the distance D4.

For angle measurements, a two-direction angle construction tool was used. Reference angles were measured using the digitally created reference plane (Plane 1) and the axis of the respective cylinder (A1, A2, A3, A4, A5). Similarly to the measurement of the



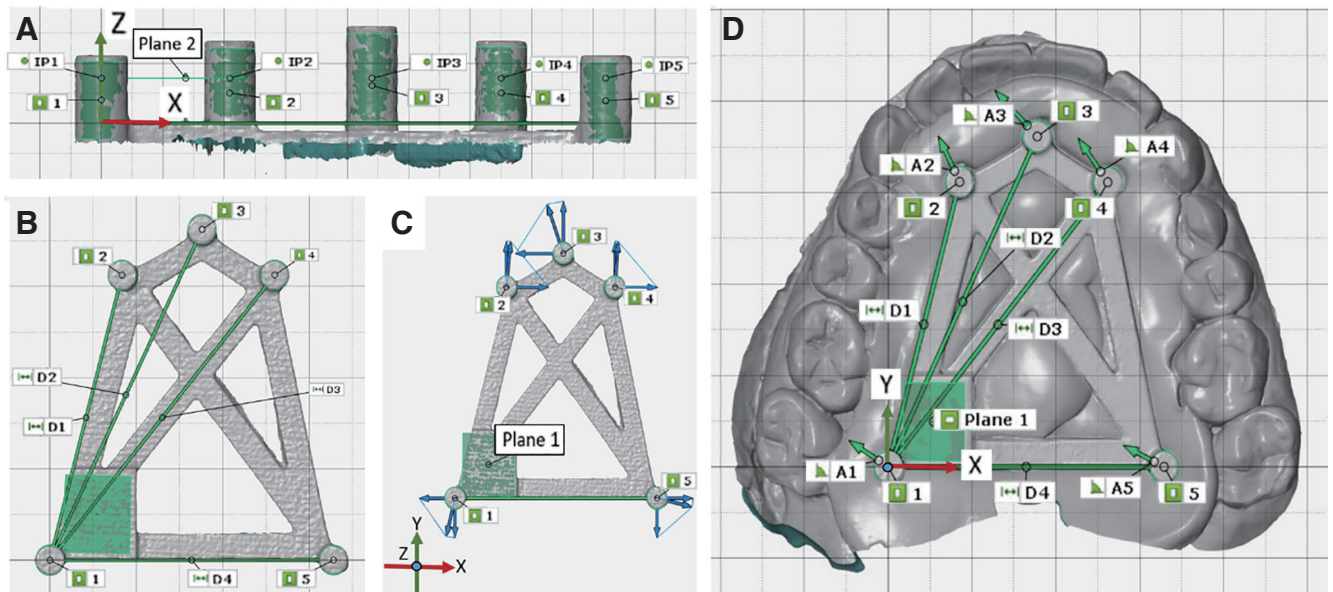


**Fig. 3.** (A) Cylinders, planes and intersection points created in each STL, (B) control distances, (C) control angles and XYZ reference system, (D) measurements in STL files acquired with IOS.

gauge at the CMM, the angles between the two elements were measured as well as their respective projections (Fig. 3). A1 was the angle between the first scanned cylinder and the digitally created reference plane (Plane 1) and A5, the angle between the last scanned cylinder and the same reference plane.

The accuracy was assessed in terms of trueness and precision according to the ISO 5725-1 standard.<sup>39</sup> Following the standard, for each reference parameter (distances D1, D2, D3 and D4 and angles A1, A2, A3, A4 and A5), the trueness was evaluated in terms of the deviations of each measurement from the reference measure, and the precision as the dispersion of measurements themselves. Both the accuracy and the trueness obtained for each reference parameter were expressed in terms of the median and interquartile range due to the asymmetry of their distribution.

Using statistical analysis software (IBM SPSS Statistics 24, IBM Corp., Armonk, NY, USA), the precision and trueness obtained for each reference parameter were compared to test the null hypothesis: there are no significant differences between the accuracy in digital impressions of a short-span area and in those of a complete arch. Therefore, a difference in the ac-

curacy (precision and trueness) obtained for the different reference parameters would lead to rejecting the null hypothesis. Furthermore, since the manufacturer's proposed scanning protocol for obtaining complete-arch digital replicas starts by scanning near the first cylinder, any reduction in the accuracy in the scanning direction (from D1 to D4 and from A1 to A5) would indicate that the digital replicas of short-span areas are more accurate than those of complete arch.

To this end, the different measurement groups (distances and angles) were compared by testing to ascertain if there were significant differences. As the assumption of normality according to the Shapiro-Wilk test was not fulfilled for the different groups, the Kruskal-Wallis test for independent samples was used. In addition, in those significance tests where statistically significant differences were detected, post-hoc pairwise comparisons were performed in order to detect where these differences exactly (between which pairwise) occurred. For that purpose, significance values adjusted by Bonferroni correction for multiple tests were used. For all comparisons, the significance level established was 0.05.

## RESULTS

Gauge measurement on the CMM yielded the reference distances and angles shown in Table 1. Having set the measurements of the reference parameters (angles and distances) and measured the same parameters in all acquired STL files, trueness and precision of digital impressions were calculated. Deviations measured in reference distances (D1, D2, D3, D4) varied from 0.01 mm to 0.132 mm in D1, from 0.002 mm to 0.158 mm in D2, from 0.014 mm to 0.143 mm in D3, and from 0.009 mm to 0.161 mm in D4. Of particular note was that in all cases the largest deviation values were measured in the same digital impression (STL7). In accordance with what was previously established, the trueness obtained at each reference distance was represented in terms of the median and the interquartile range of these deviations. It is worth noting that the best trueness values were obtained in D1 reference distance while the worst values were obtained in D4, ranging from  $0.018 \pm 0.021$  mm in D1 to  $0.106 \pm 0.08$  mm in D4. All values are summarized in

Table 2.

In addition to trueness, precision was analyzed. Calculated values ranged from 0.004 mm to 0.108 mm in D1, from 0 to 0.136 mm in D2, from 0.005 mm to 0.106 mm in D3, and from 0.021 mm to 0.176 mm in D4. Similar to trueness, the precision obtained at each reference distance was represented in terms of the median and the interquartile range of these deviations. In this case again, the highest precision was calculated in D1 reference distance while the lowest values were in D4 (Fig. 4). They ranged from  $0.015 \pm 0.03$  mm in D1 to  $0.077 \pm 0.073$  mm in D4. Table 3 summarizes precision values for each reference distance.

When comparing different distance groups, the Kruskal-Wallis test yielded significant differences in both trueness and precision. According to the results obtained in the post-hoc pairwise comparisons, these differences were found in both cases between the reference distances D1 and D4 (Table 4). The boxplots represented in Fig. 4 highlight the mentioned outcomes.

Regarding the angle measurements, three groups of

**Table 1.** Reference distances and angles measured in the gauge using the CMM

Reference parameters			
Reference distances	Distance (mm)		
D1	32.305		
D2	40.263		
D3	40.622		
D4	32.804		
Reference angles	Angle with XY	Projection on YZ	Projection on ZX
A1	89:49:33	-89:56:27	89:49:06
A2	-89:53:48	-89:53:50	89:59:18
A3	-89:56:10	-89:59:13	-89:56:15
A4	-89:55:50	-89:57:36	-89:56:36
A5	-89:51:59	-89:54:10	-89:54:30

**Table 2.** Trueness in distance groups

Distance group	Mean	95% Confidence Interval for Mean		Median	Std. deviation	Interquartile range	
		Lower bound	Upper bound				
Trueness (mm)	D1	0.031	0.005	0.057	0.018	0.037	0.021
	D2	0.039	0.008	0.071	0.027	0.044	0.026
	D3	0.053	0.025	0.080	0.041	0.038	0.047
	D4	0.095	0.057	0.133	0.106	0.053	0.080

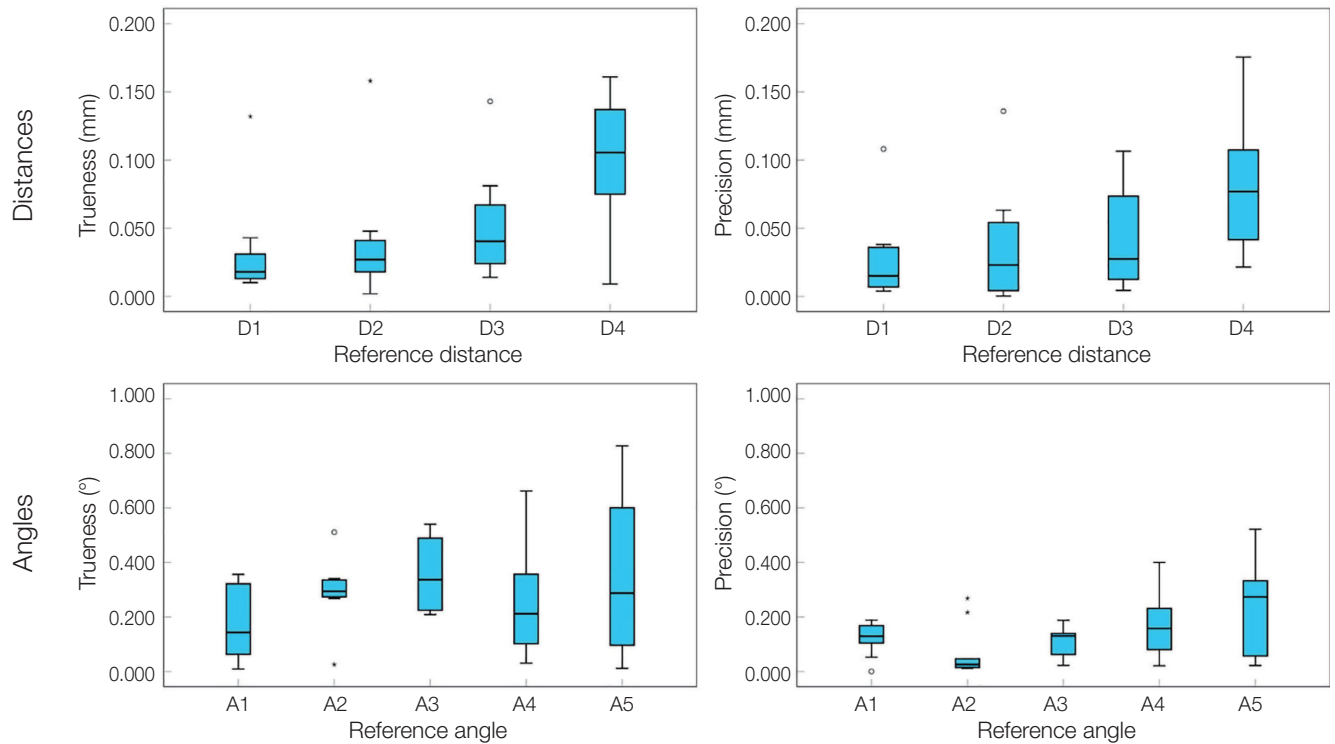


**Fig. 4.** Trueness and precision in reference distances and reference angles with respect to the XY plane.

**Table 3.** Precision in distance groups

Distance group	Mean	95% Confidence Interval for Mean		Median	Std. deviation	Interquartile range	
		Lower bound	Upper bound				
Precision (mm)	D1	0.027	0.004	0.049	0.015	0.032	0.030
	D2	0.035	0.006	0.065	0.023	0.041	0.053
	D3	0.041	0.017	0.066	0.028	0.034	0.063
	D4	0.082	0.048	0.115	0.077	0.047	0.073

**Table 4.** Pairwise comparisons of distance groups

Sample 1-Sample 2	Trueness Bonferroni adjusted Sig.	Precision Bonferroni adjusted Sig.
D1-D2	1.000	1.000
D1-D3	0.406	1.000
D1-D4	0.035	0.023
D2-D3	1.000	1.000
D2-D4	0.313	0.062
D3-D4	1.000	0.350

results were obtained: 1) angles of the cylinders with respect to the XY plane - the value of the angle in real magnitude; 2) the projections of the angles in the YZ plane; and 3) the projections of the angles in the ZX plane.

Measurements of angles in the XY plane yielded low values of deviation from the reference measures. All were lower than 0.9°. They ranged from 0.009° in A1 reference angle, measured in STL6, to 0.827° in A5 and measured in STL1. In addition, and contrarily to distances analysis, angle measurement did not show a tendency to rise when the scanning length increased.

**Table 5.** Trueness in XY angle group

Angle group	Mean	95% Confidence Interval for Mean		Median	Std. deviation	Interquartile range	
		Lower bound	Upper bound				
Trueness (°)	A1	0.173	0.075	0.272	0.143	0.138	0.273
	A2	0.294	0.210	0.379	0.294	0.118	0.064
	A3	0.353	0.262	0.443	0.337	0.126	0.266
	A4	0.263	0.107	0.418	0.212	0.217	0.322
	A5	0.327	0.127	0.527	0.288	0.280	0.525

**Table 6.** Precision in XY angle group

Angle group	Mean	95% Confidence Interval for Mean		Median	Std. deviation	Interquartile range	
		Lower bound	Upper bound				
Precision (°)	A1	0.122	0.079	0.166	0.129	0.061	0.081
	A2	0.068	0.002	0.135	0.026	0.093	0.075
	A3	0.110	0.074	0.146	0.130	0.050	0.080
	A4	0.173	0.088	0.257	0.157	0.118	0.175
	A5	0.245	0.129	0.362	0.274	0.163	0.296

Nor were particularly offset values measured in STL7. It is also noticeable that in 48 of the 50 measurements the deviations were in the positive range. Trueness values obtained from these deviations moved from  $0.143 \pm 0.273^\circ$  in A1 to  $0.337 \pm 0.266^\circ$  in A3. Table 5 compiles all calculated trueness values of the angles with respect to the XY planes.

Calculated precision values were also low. All were below  $0.6^\circ$ , with the lowest 0 on A1, measured in STL9, and the highest  $0.522^\circ$  on A5, measured in STL1. With these calculated deviations, precision values ranged from  $0.026 \pm 0.075^\circ$  in A2 to  $0.274 \pm 0.296^\circ$  in A5. Precision values in each reference angle measured in the XY plane are shown in Table 6.

In the case of angles with respect to the XY plane, the Kruskal-Wallis test showed significant differences between the precision values obtained in the different reference angle groups, but not between the trueness values. For precision, according to the results obtained in the post-hoc pairwise comparisons, the differences were found between reference angles A2 and A5 (Table 7). Boxplots on Fig. 4 show graphically the trueness and precision of angle measurements

**Table 7.** Pairwise comparisons of angles with respect to the XY plane groups

Sample 1-Sample 2	Precision Bonferroni adjusted Sig.
A2-A3	1.000
A2-A1	0.858
A2-A4	0.124
A2-A5	0.010
A3-A1	1.000
A3-A4	1.000
A3-A5	0.592
A1-A4	1.000
A1-A5	1.000
A4-A5	1.000

with respect to the XY plane and the non-existent trend of growth that was evident in the analysis of the distances.

The behavior of the deviations of angles projected in the YZ and ZX planes was similar to that of the angle measurement in its real magnitude (XY plane).



Trueness values ranged from  $0.078 \pm 0.283^\circ$  in A5 projected in the YZ plane, to  $0.252 \pm 218^\circ$  in A2 and projected in the ZX plane. Precision varied from  $0.059 \pm 0.06^\circ$  in A1 projected in the YZ plane to  $0.196 \pm 0.229^\circ$  in A5 and projected in the ZX plane. No deviation value higher than  $0.3^\circ$  was calculated. All calculated values are summarized in Tables 8-11. In accordance with these results, Kruskal-Wallis test did not show

significant differences for trueness and precision values between different reference angles groups. Box-plots in Fig. 5 show graphically the results obtained and, as with the boxplot that showed the deviations for the angles with respect to XY, in this case they also did not show trends of worsening when the scanning area increased.

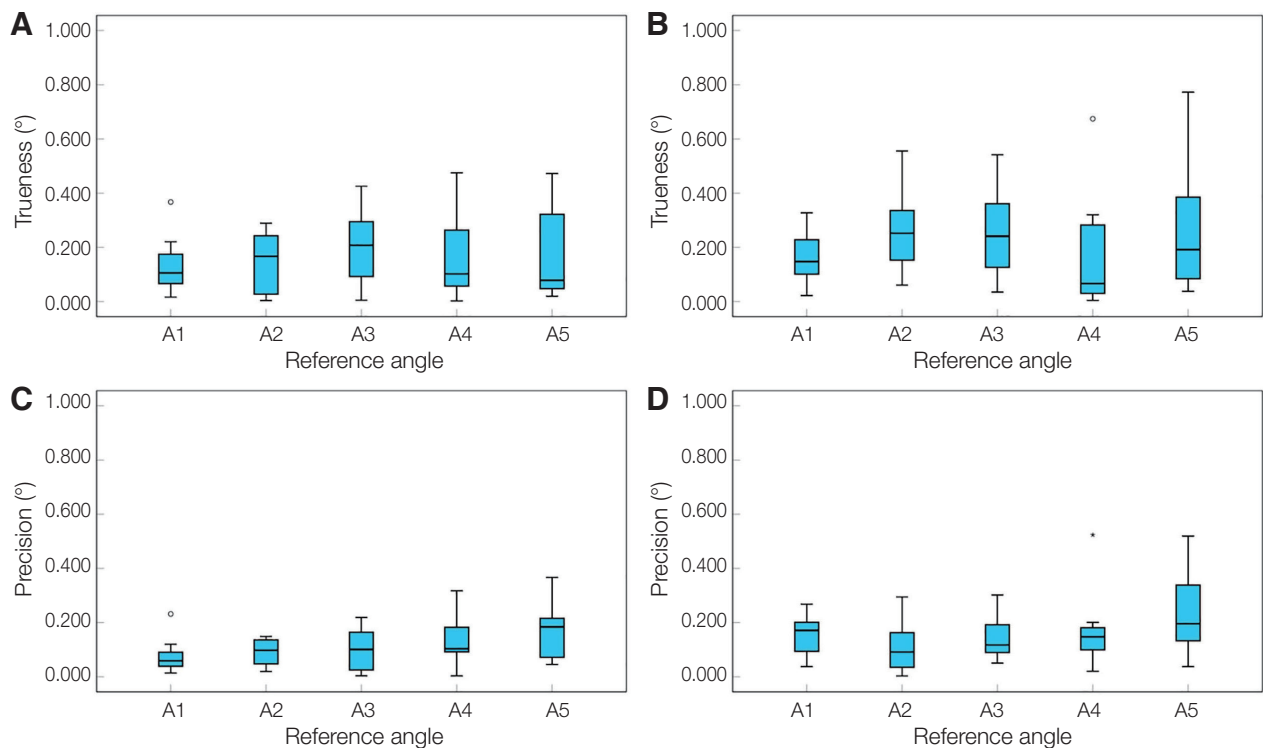


**Fig. 5.** (A) Trueness of angles on YZ plane, (B) trueness of angles on ZX plane, (C) precision of angles on YZ, (D) precision of angles on ZX.

**Table 8.** Trueness in YZ projection angle group

Angle group (YZ projection)	Statistic						
	Mean	95% Confidence Interval for Mean		Median	Std. deviation	Interquartile range	
		Lower bound	Upper bound				
Trueness (°)	A1	0.136	0.062	0.209	0.105	0.103	0.125
	A2	0.153	0.075	0.231	0.167	0.109	0.225
	A3	0.215	0.117	0.312	0.208	0.137	0.232
	A4	0.163	0.048	0.278	0.102	0.161	0.245
	A5	0.154	0.039	0.270	0.078	0.162	0.283

**Table 9.** Precision in YZ projection angle group

Angle group (YZ projection)	Mean	95% Confidence Interval for Mean		Median	Std. deviation	Interquartile range	
		Lower bound	Upper bound				
Precision (°)	A1	0.078	0.033	0.123	0.059	0.063	0.060
	A2	0.093	0.058	0.127	0.098	0.049	0.097
	A3	0.107	0.049	0.164	0.101	0.080	0.155
	A4	0.130	0.063	0.197	0.103	0.094	0.119
	A5	0.164	0.093	0.236	0.184	0.100	0.153

**Table 10.** Trueness in ZX projection angle group

Angle group (ZX projection)	Mean	95% Confidence Interval for Mean		Median	Std. deviation	Interquartile range	
		Lower bound	Upper bound				
Trueness (°)	A1	0.155	0.091	0.220	0.147	0.090	0.139
	A2	0.261	0.153	0.368	0.252	0.150	0.218
	A3	0.246	0.128	0.365	0.241	0.166	0.265
	A4	0.168	0.017	0.318	0.067	0.210	0.266
	A5	0.287	0.098	0.475	0.192	0.264	0.375

**Table 11.** Precision in ZX projection angle group

Angle group (ZX projection)	Mean	95% Confidence Interval for Mean		Median	Std. deviation	Interquartile range	
		Lower bound	Upper bound				
Precision (°)	A1	0.151	0.097	0.205	0.171	0.075	0.124
	A2	0.113	0.048	0.179	0.092	0.091	0.141
	A3	0.146	0.084	0.208	0.117	0.087	0.132
	A4	0.169	0.072	0.266	0.147	0.136	0.094
	A5	0.245	0.137	0.354	0.196	0.152	0.229

## DISCUSSION

In the present study, a new methodology to assess the accuracy of IOS was tested. In line with ISO 12836:2015,<sup>37</sup> which describes test methods for assessing accuracy of dental scanners, the basis of the methodology was the use of a calibrated element. This calibrated element was used to compare measurements acquired from the digital impressions obtained with IOS with reference measurements of the calibrated element.

The use of calibrated elements, as well as basic

geometric figures, has already been proposed for IOS accuracy analysis.<sup>26,27,35,38</sup> However, most published works in this field have relied on best-fit alignment methods, which are based on the superimposition of digitally acquired meshes.<sup>14,18,20,21,24,26</sup> This superimposition is performed by the software itself seeking minimum deviation between aligned meshes. When analyzing deviations between these aligned meshes, the results yielded by the software are the distances between a point on the reference mesh and any point that is the closest in the analysis mesh. That is,

it may be giving deviations between two points that are not actually the digital replica of the same point. These methods are indeed valid to assess accuracy in specific clinical cases or applications; nonetheless, the use of an external element such as a calibrated gauge enables the definition of an exact point on the reference mesh and comparison with the same point on the mesh under analysis. These comparisons may provide useful data for assessing the scanner's accuracy. However, to normalize the use of a gauge, it must meet certain conditions. It must have been manufactured to exacting geometrical and dimensional tolerances and have high surface qualities. The gauge designed and manufactured for this study does not meet these conditions since the objective was to test the validity of the methodology. In addition, after the milling, the gauge was shot-blasted to avoid reflections, which could have altered the surfaces of the gauge, thus enhancing the flatness of the reference plane or the cylindricity of the cylinders. Nor can it be guaranteed that the gauge can be placed in any mouth, since the dimensions of 5 mouths have been taken into account in its design. The manufacture of a definitive gauge requires a certain methodological acceptance of the process of assessing the accuracy of the IOS.

In order to test the validity of this method, it was applied in the accuracy study of a well-known IOS, and trueness and precision of acquired digital impressions were analyzed. The null hypothesis stated that the distribution of trueness and precision was the same across categories of distance and angle groups. In the distance group, as can be seen in the boxplots shown in Figure 4, the independent-samples Kruskal-Wallis test rejected this hypothesis with 0.035 and 0.018 values, respectively; the accuracy and precision were both influenced by the scanned arch length. However, results were not as conclusive concerning angle measurements. The Kruskal-Wallis test showed that there were no significant differences in almost all analyzed cases. Only when analyzing precision of angle measurement with the XY plane did the test yield a significance lower than 0.05. For all other comparisons, both with regard to trueness and precision, no differences were found.

This different behavior when analyzing errors in dis-

tances or angles may be due to one of the limitations of this study. The mere fact of using a gauge influences the scanning results. The scanners create a 3D image by stitching together multiple camera captures, and to perform these stitching operations, they rely on geometric references or colors. The use of a gauge provides the scanner with an element on which to rely to join the multiple image captures. The designed gauge has the cylinders joined together with a prismatic structure. The fact that the cylinders are connected with a continuous and rectangular section geometry might assist the scanner in preventing the rotation of the multiple captures it takes, thus avoiding angle errors. Although the use of any external element, such as a measuring gauge, always influences the results on accuracy analysis, it would be interesting to explore this further and try to minimize its influence.

The proposed methodology also has other limitations. In accordance with the aforementioned benefit that the gauge may provide, one of the limitations is the fact that the study was carried out in a dentulous patient. The denture provides geometric references that facilitate the creation of the 3D image. An edentulous jaw, presumably, would yield worse results, as has been mentioned in other literature.<sup>8,31</sup>

With regard to the obtained results, the IOS showed high accuracy in short-span areas of the dental arch while accuracy decreased as the length of the arch was increased. This behavior has been revealed in several studies.<sup>8,23,27</sup> It is worth highlighting that the worst deviation value when analyzing distance did not reach 0.2 mm. In both trueness and precision calculations, values in all cases were under 0.1 mm. It is logical that the results are influenced by which scanner is used, though they are slightly lower than those obtained in other *in vitro* studies.<sup>38</sup> It should be noted as another limitation, that only one intraoral scanner was used to test the proposed methodology and it is predictable that the accuracy will vary if other scanners were used.

When analyzing angles, measured deviations were minor. Deviation values when analyzing trueness were below 0.6°, which is within the Andriessen recommendation,<sup>31</sup> and when analyzing precision, all values were below 0.9°. Nevertheless, the fact that

the behavior of the evolution of the error along the dental arch is different from that of the error in the distance forces a reconsideration of the validity of the gauge to analyze angulation errors. It is possible that the geometry of the gauge or even its placement in the mouth could have influenced the results.

A further interesting aspect of this study is that it was carried out *in vivo*. IOS are designed to be used in the mouth so studies of their validity should be carried out in the mouth. It was expected that results would be worse than in *in vitro* studies, but in fact they were in line with other studies. Certainly, for this study, the gauge was placed in the maxilla and not in the lower jaw, which would pose a significantly added difficulty. The tongue does not allow the gauge to be placed in the lower arch. Consequently, if there were larger errors when scanning the lower jaw, they would be derived from the difficulty of the scan itself rather than from the nature or capacity of the scanner, which is also what occurs with replicas obtained following conventional methods, using alginates to make plaster models.

In recent years, numerous studies have been published concerning the accuracy of IOS. The vast majority have focused on measuring deviations in specific clinical cases or differences between superimposed meshes. However, there is no general and common criterion to determine the accuracy of an IOS. This circumstance is similar to that of non-contact optical scanners used in other fields, such as industry, and because of this, efforts are being directed at establishing such criteria. Apparently, the formulas for establishing a valid methodology for measuring the accuracy of optical scanners will come from the use of gauges and so this is proposed in ISO 12836: 2015<sup>37</sup>. The methodology presented in this study is in this direction.

## CONCLUSION

It is possible to analyze the accuracy of IOS *in vivo*. The current study presents an approach based on the use of a feature-based gauge that enables the assessment of trueness and precision. Moreover, both trueness and precision can be measured for different arch lengths. Results confirm that the digital impression

showed poorer accuracy as the length of the scanned arch increases. The trueness and accuracy values for distances up to half-arch, including incisors, did not reach 0.05 mm (median value). For the full arch, these deviations almost tripled.

## ACKNOWLEDGEMENTS

The authors thank Dr Raúl Diéz of the RD Orthodontic and Pediatric Dentistry Clinic, Naiara Ortega of the Mechanics Department of the University of the Basque Country (UPV/EHU) and of the CFAA, The Aeronautics Advanced Manufacturing Center (<https://www.ehu.eus/en/web/cfaa/>) for their support and assistance in the conduct of this research work.

## REFERENCES

1. Ahrberg D, Lauer HC, Ahrberg M, Weigl P. Evaluation of fit and efficiency of CAD/CAM fabricated all-ceramic restorations based on direct and indirect digitalization: a double-blinded, randomized clinical trial. *Clin Oral Investig* 2016;20:291-300.
2. Joda T, Brägger U. Digital vs. conventional implant prosthetic workflows: a cost/time analysis. *Clin Oral Implants Res* 2015;26:1430-5.
3. Lee SJ, Gallucci GO. Digital vs. conventional implant impressions: efficiency outcomes. *Clin Oral Implants Res* 2013;24:111-5.
4. Patzelt SB, Lamprinos C, Stampf S, Att W. The time efficiency of intraoral scanners: an in vitro comparative study. *J Am Dent Assoc* 2014;145:542-51.
5. Marghalani A, Weber HP, Finkelman M, Kudara Y, El Rafie K, Papaspyridakos P. Digital versus conventional implant impressions for partially edentulous arches: An evaluation of accuracy. *J Prosthet Dent* 2018;119:574-9.
6. Renne W, Ludlow M, Fryml J, Schurch Z, Mennito A, Kessler R, Lauer A. Evaluation of the accuracy of 7 digital scanners: An in vitro analysis based on 3-dimensional comparisons. *J Prosthet Dent* 2017;118:36-42.
7. Gjelvold B, Chrcanovic BR, Korduner EK, Collin-Bagevitz I, Kisch J. Intraoral digital impression technique compared to conventional impression technique. A randomized clinical trial. *J Prosthodont* 2016;25:282-7.

8. Iturrate M, Eguiraun H, Solaberrieta E. Accuracy of digital impressions for implant-supported complete-arch prosthesis, using an auxiliary geometry part-an in vitro study. *Clin Oral Implants Res* 2019;30:1250-8.
9. Luo H, Xu J, Hoa Binh N, Liu S, Zhang C, Chen K. A simple calibration procedure for structured light system. *Opt Lasers Eng* 2014;57:6-12.
10. Martínez-Pellitero S, Cuesta E, Giganto S, Barreiro J. New procedure for qualification of structured light 3D scanners using an optical feature-based gauge. *Opt Lasers Eng* 2018;110:193-206.
11. Revilla-León M, Jiang P, Sadeghpour M, Piedra-Cascón W, Zandinejad A, Özcan M, Krishnamurthy VR. Intraoral digital scans-Part 1: influence of ambient scanning light conditions on the accuracy (trueness and precision) of different intraoral scanners. *J Prosthet Dent* 2020;124:372-8.
12. Dury MR, Woodward SD, Brown SB, McCarthy MB. Surface finish and 3D optical scanner measurement performance for precision engineering. *Proc - ASPE 2016 Annu Meet* 2016;167-72.
13. Chen Y, Zhai Z, Li H, Yamada S, Matsuoka T, Ono S, Nakano T. Influence of liquid on the tooth surface on the accuracy of intraoral scanners: an in vitro study. *J Prosthodont* 2021 Apr 7. doi: 10.1111/jopr.13358.
14. Imburgia M, Logozzo S, Hauschild U, Veronesi G, Mangano C, Mangano FG. Accuracy of four intraoral scanners in oral implantology: a comparative in vitro study. *BMC Oral Health* 2017;17:92.
15. Aragón ML, Pontes LF, Bichara LM, Flores-Mir C, Normando D. Validity and reliability of intraoral scanners compared to conventional gypsum models measurements: a systematic review. *Eur J Orthod* 2016;38:429-34.
16. Lim JH, Park JM, Kim M, Heo SJ, Myung JY. Comparison of digital intraoral scanner reproducibility and image trueness considering repetitive experience. *J Prosthet Dent* 2018;119:225-32.
17. Fukazawa S, Odaira C, Kondo H. Investigation of accuracy and reproducibility of abutment position by intraoral scanners. *J Prosthodont Res* 2017;61:450-9.
18. Güth JF, Runkel C, Beuer F, Stimmelmayer M, Edelhoff D, Keul C. Accuracy of five intraoral scanners compared to indirect digitalization. *Clin Oral Investig* 2017; 21:1445-55.
19. Hack GD, Patzelt SBM. Evaluation of the accuracy of six intraoral scanning devices: an in-vitro investigation. *Am Dent Assoc* 2015;10:1-5.
20. Ali AO. Accuracy of digital impressions achieved from five different digital impression systems. *Dentistry* 2015;5:300.
21. Patzelt SB, Emmanouilidi A, Stampf S, Strub JR, Att W. Accuracy of full-arch scans using intraoral scanners. *Clin Oral Investig* 2014;18:1687-94.
22. Patzelt SB, Bishti S, Stampf S, Att W. Accuracy of computer-aided design/computer-aided manufacturing-generated dental casts based on intraoral scanner data. *J Am Dent Assoc* 2014;145:1133-40.
23. Ender A, Mehl A. Accuracy of complete-arch dental impressions: a new method of measuring trueness and precision. *J Prosthet Dent* 2013;109:121-8.
24. Ender A, Mehl A. In-vitro evaluation of the accuracy of conventional and digital methods of obtaining full-arch dental impressions. *Quintessence Int* 2015;46:9-17.
25. Mangano FG, Admakin O, Bonacina M, Lerner H, Rutkunas V, Mangano C. Trueness of 12 intraoral scanners in the full-arch implant impression: a comparative in vitro study. *BMC Oral Health* 2020;20:263.
26. van der Meer WJ, Andriessen FS, Wismeijer D, Ren Y. Application of intra-oral dental scanners in the digital workflow of implantology. *PLoS One* 2012;7:e43312.
27. Güth JF, Edelhoff D, Schweiger J, Keul C. A new method for the evaluation of the accuracy of full-arch digital impressions in vitro. *Clin Oral Investig* 2016;20: 1487-94.
28. Syrek A, Reich G, Ranftl D, Klein C, Cerny B, Brodesser J. Clinical evaluation of all-ceramic crowns fabricated from intraoral digital impressions based on the principle of active wavefront sampling. *J Dent* 2010;38:553-9.
29. Pradíes G, Zarauz C, Valverde A, Ferreiroa A, Martínez-Rus F. Clinical evaluation comparing the fit of all-ceramic crowns obtained from silicone and digital intraoral impressions based on wavefront sampling technology. *J Dent* 2015;43:201-8.
30. Ender A, Zimmermann M, Attin T, Mehl A. In vivo precision of conventional and digital methods for obtaining quadrant dental impressions. *Clin Oral Investig* 2016;20:1495-504.
31. Andriessen FS, Rijkens DR, van der Meer WJ, Wismeijer DW. Applicability and accuracy of an intraoral scanner



- for scanning multiple implants in edentulous mandibles: a pilot study. *J Prosthet Dent* 2014;111:186-94.
32. Ender A, Attin T, Mehl A. In vivo precision of conventional and digital methods of obtaining complete-arch dental impressions. *J Prosthet Dent* 2016;115:313-20.
  33. Zhang F, Suh KJ, Lee KM. Validity of intraoral scans compared with plaster models: an in-vivo comparison of dental measurements and 3D surface analysis. *PLoS One* 2016;11:e0157713.
  34. Zimmermann M, Koller C, Rumetsch M, Ender A, Mehl A. Precision of guided scanning procedures for full-arch digital impressions in vivo. *J Orofac Orthop* 2017;78:466-471.
  35. Kuhr F, Schmidt A, Rehmann P, Wöstmann B. A new method for assessing the accuracy of full arch impressions in patients. *J Dent* 2016;55:68-74.
  36. Pan Y, Tam JM, Tsoi JK, Lam WY, Huang R, Chen Z, Pow EH. Evaluation of laboratory scanner accuracy by a novel calibration block for complete-arch implant rehabilitation. *J Dent* 2020;102:103476.
  37. ISO 12836. Dentistry - Digitizing devices for CAD/CAM systems for indirect dental restorations - test methods for assessing accuracy. International Standards Organization (ISO); Geneva; Switzerland, 2015. Available at: <https://www.iso.org/standard/68414.html> Accessed July 15, 2021.
  38. Iturrate M, Lizundia E, Amezua X, Solaberrieta E. A new method to measure the accuracy of intraoral scanners along the complete dental arch: a pilot study. *J Adv Prosthodont* 2019;11:331-40.
  39. ISO 5725-1. Accuracy (trueness and precision) of measurement methods and results - Part 1: General principles and definitions. International Standards Organization (ISO); Geneva; Switzerland, 1994. Available at: <https://www.iso.org/standard/11833.html> Accessed August 4, 2021.